OLEFIN SELECTIVE CARBON-SUPPORTED K-Fe-Mn CO HYDROGENATION CATALYSTS: A KINETIC, CALORIMETRIC, CHEMISORPTION, INFRARED AND MÖSSBAUER SPECTROSCOPIC INVESTIGATION

Jeremy J. VENTER [1,*] and M. Albert VANNICE [2]

[1] *Rohm & Haas Company, 727 Norristown Road, Spring House, PA 19477, U.S.A.*
[2] *Department of Chemical Engineering, The Pennsylvania State University, University Park, PA 16802, U.S.A.*

Carbon supported Fe, Fe-Mn, K-Fe-Mn catalysts, mixed metal carboxyl clusters, chemisorption, kinetic measurements, calorimetric measurements, infrared spectroscopy, Mössbauer spectroscopy

Carbon-supported Fe, Fe-Mn, and K-Fe-Mn catalysts derived from stoichiometric mixed-metal carbonyl clusters were pretreated at either 473 K or 673 K in hydrogen. Chemisorption and kinetic measurements were conducted following these pretreatments. The iron remained highly dispersed at all times except after high temperature reductions when potassium was present. The single promotion by either Mn or K increases the olefin/paraffin ratio, while the doubly promoted catalyst gave very high selectivities for light olefins. Isothermal, integral heats of adsorption of CO were determined at 300 K, and they increased from 15 kcal/mole for Fe_3/C to nearly 17 kcal/mole for both the singly promoted Fe_2Mn/C and KFe_3/C catalysts to 21 kcal/mole for the doubly promoted KFe_2Mn/C sample. A model of the decomposition of these carbonyl clusters is proposed based on calorimetric, Mössbauer effect spectroscopic and diffuse reflectance Fourier transform infrared spectroscopic studies. The state of the MnO_x and K phases on the iron surface, as well as the Fe crystallite size, appears to play a dominant role in determining the catalytic behavior.

1. Introduction

A number of reports have appeared describing the intriguing catalytic properties of Fe-Mn catalysts, namely the high activities and olefin selectivities in CO hydrogenation reactions. The reasons for this enhancement in activities and selectivities are not clear. The catalysts most frequently studied are Fe-Mn mixed oxides [1–15]. Relatively few studies focussing on the properties of highly dispersed Fe-Mn and K-Fe-Mn catalysts exist [16–18]. An initial study of highly dispersed carbon-supported Fe, Fe-Mn, and K-Fe-Mn catalysts revealed that these favorable properties could be reproduced, and even improved upon [18].

* To whom correspondence should be addressed.

This earlier study prompted a very thorough characterization of carbon-supported Fe-Mn and K-Fe-Mn catalysts, prepared from mixed metal clusters (MMC's).

The interest in these catalysts stems from the fact that highly active carbon-supported catalysts can be prepared, while maintaining the high selectivities to low molecular weight olefins. Catalysts can be prepared with activities, on a per gram Fe basis, higher than those reported for bulk Fe-Mn catalysts. The metal precursors used were metal carbonyl clusters. These clusters allow the ready preparation of precursor materials containing the metals of interest, including K, in the desired stoichiometric ratios. Since the metals in these clusters are in a low oxidation state, only mild reductions are required to produce active catalysts. Furthermore, using carbon as a support material allows the stabilization of highly dispersed metals, and characterizing these CO hydrogenation catalysts using a broad range of techniques, including CO chemisorption, diffuse reflectance infrared Fourier transform spectroscopy (DRIFTS), Mössbauer effect spectroscopy (MES), transmission electron microscopy/energy dispersive spectroscopy (TEM/EDS), and differential scanning calorimetry (DSC). These techniques allowed us to follow the decomposition of the original clusters on the carbon support, to characterize the catalysts following low and high temperature reductions, and also to study their kinetic behaviour in the CO hydrogenation reaction. These results were used in an attempt to correlate the physical state of the K-Fe-Mn/C catalysts to their kinetic properties. These results were fully described in a recent series of publications [19–21]. The purpose of the current publication is to summarize these results, and to show the correlation between the surface and bulk states of these highly dispersed metals and their catalytic performance.

2. Experimental

The catalysts and their preparation without air exposure from $Fe_3(CO)_{12}$, $Mn_2(CO)_{10}$, $NEt_4[Fe_2Mn(CO)_{12}]$, $K[Fe_2Mn(CO)_{12}]$, $K[FeMn(CO)_9]$, and $K[HFe_3(CO)_{11}]$ using Schlenk line techniques are described elsewhere [18,19,22]. These catalysts will be abbreviated as Fe_3/C, Mn_2/C, Fe_2Mn/C, KFe_2Mn/C, KFeMn/C, and KFe_3, respectively.

The equipment used for the chemisorption, kinetic, and calorimetric measurements was described previously [19,20,23]. Chemisorption of CO on the fresh catalysts was measured after a low temperature reduction (LTR) for 2 hours in H_2 at 473 K as well as after a high temperature reduction (HTR) for 16 hours in H_2 at 673 K. The used samples (after the kinetic runs) were evaluated after the HTR step only. Details are given elsewhere [24,25]. CO chemisorption was determined using a dual isotherm method [26]. The kinetic measurements were obtained at 1 atm under differential conditions using a glass, plug-flow reactor [18]. The activities for CO hydrogenation were obtained after either the LTR or

the HTR step by using a bracketing technique to avoid deactivation [27], and partial pressure dependencies studies were obtained by using a power rate law and varying the partial pressures of CO and H_2 with He as diluent gas [18]. The isothermal energy changes during CO adsorption were measured in a modified Perkin-Elmer DSC-2C differential scanning calorimeter, as described previously [23,28]. The MES apparatus and experimental procedures are described elsewhere [20,29].

3. Results and discussion

A: KINETIC, CHEMISORPTION, AND CALORIMETRIC STUDY

Bulk Fe-Mn and K-Fe-Mn oxide catalysts have been reported to have high selectivities for the formation of low molecular weight olefins while maintaining high activities [1–15]. Very few reports existed in the literature at the inception of this study dealing with the preparation and characterization of highly dispersed, supported Fe-Mn and K-Fe-Mn catalysts [16,17] although these catalysts were reported to be active and olefin selective. The characterization of these two series of catalysts consisted of determining the weight loadings and estimating the dispersions of the supported metals. As these catalysts are olefin selective, highly dispersed supported Fe-Mn and K-Fe-Mn catalysts provide a unique opportunity to study the physical characteristics of the supported metals and to attempt to relate these properties to the catalytic performance. Because the materials are highly dispersed, a large fraction of the metal atoms are on the surface. This should further enable the desirable observations to be made.

An initial study was done in this laboratory to determine if the catalytic properties of the K-Fe-Mn system could be reproduced when these metals are supported on oxygen-free carbon to eliminate the interaction of Fe, Mn, and K with oxide surfaces [18]. Metal carbonyl clusters (MCC's) were used as the metal precursors, and supported on a high surface area carbon black. The carbon was thoroughly desulfurized by heating in H_2 at 1273 K, which also removed surface functional groups, and then dried prior to impregnation [18]. Highly dispersed metal catalysts were prepared and full details of the catalyst preparations and kinetic evaluations are given elsewhere [18]. A list of the metal precursors is given in table 1. Metal carbonyl clusters were mainly used, with Fe-to-Mn molar ratios varing from 2-to-1 to 1-to-2, and metal weight loadings between 1 and 4%. $Mn_2(CO)_{10}$ and $Fe_3(CO)_{12}$ were also supported and evaluated, both individually and co-impregnated to yield similar Fe-to-Mn ratios, as mentioned. Three potassium promoted catalysts using mixed metal MCC's as precursors were prepared. The catalysts prepared in this earlier study were evaluated at atmospheric pressure, 548 K, and with a H_2-to-CO ratio of 3. The activities and selectivities of these catalysts were compared to a number of catalysts reported in the literature. The catalysts prepared by Barrault et al. [7,30,31], Bruce et al. [16], Deckwer et al.

Table 1
Metal carbonyl clusters used as precursors in the preparation of carbon-supported Fe-Mn and K-Fe-Mn catalysts

Cluster precursor	Designation
$Mn_2(CO)_{10}$	Mn_2
$Mn_2Fe(CO)_{14}$	Mn_2Fe
$NEt_4[MnFe(CO)_9]$	MnFe
$NEt_4[MnFe_2(CO)_{12}]$	$MnFe_2$
$Fe_3(CO)_{12}$	Fe_3
$K[MnFe(CO)_9]$	KMnFe
$K[MnFe_2(CO)_{12}]$	$KMnFe_2$
$K[HFe_3(CO)_{11}]$	KFe_3
$Mn_2(CO)_{10} + Fe_3(CO)_{12}$	2Mn/Fe
$Mn_2(CO)_{10} + Fe_3(CO)_{12}$	Mn/2Fe
$Fe(NO_3)_3 + Mn(NO_3)_2$)	Mn/2Fe-nitrates

[32,33], Van Dijk et al. [34], Satterfield et al. [35,36], Schulz et al. [37–39], and Kuznetsov et al. [17] were evaluated at the conditions shown in table 2. The catalytic activities and selectivities of these catalysts are summarized in fig. 1. Clearly, the activities of the carbon-supported K-Fe-Mn catalysts were comparable to those reported elsewhere when compared on a per mole Fe basis. Similarly, the olefin selectivities of the carbon-supported catalysts were comparable, and in some cases higher, than those reported in the literature.

A new series of catalysts was prepared for the physical characterization experiments. As described elsewhere [19–21], the catalysts were prepared using identical procedures as for the catalysts above, but higher loadings of metals were utilized. This series included a single Fe-Mn/C catalyst, namely one with an Fe-to-Mn ratio of 2, and this catalyst had the highest olefin selectivity of the

Table 2
A comparison of carbon-supported Fe-Mn and K-Fe-Mn catalysts to bulk, and oxide-supported Fe-Mn catalysts: reaction conditions and catalyst description (Coppt = prepared by Coprecipitation Techniques)

Study	Catalyst	Mn/Fe ratio	P (atm)	T (°C)	H_2/CO (moles)
Venter et al.	Fe-Mn/C	0–2	1	275	3
1. Barrault et al.	Fe^0-Fe^{3+}/MnO, MnO_2	High	1	280	1
2. Bruce et al.	$MnFe_2/SiO_2$	0.5	2–5	300	1.5
3. Deckwer et al.	Bulk, Coppt	11	2	290	0.6
4. Van Dijk et al.	Bulk, Coppt	1.5	1	240	1
5. Satterfield et al.	Bulk, Coppt	7.3	11	280	0.8
6. Schulz et al.	Bulk, Coppt	2–23	10	250	1.9
7. Kuznetsov et al.	$MnFe_2$/oxides	0.5	1	250	2

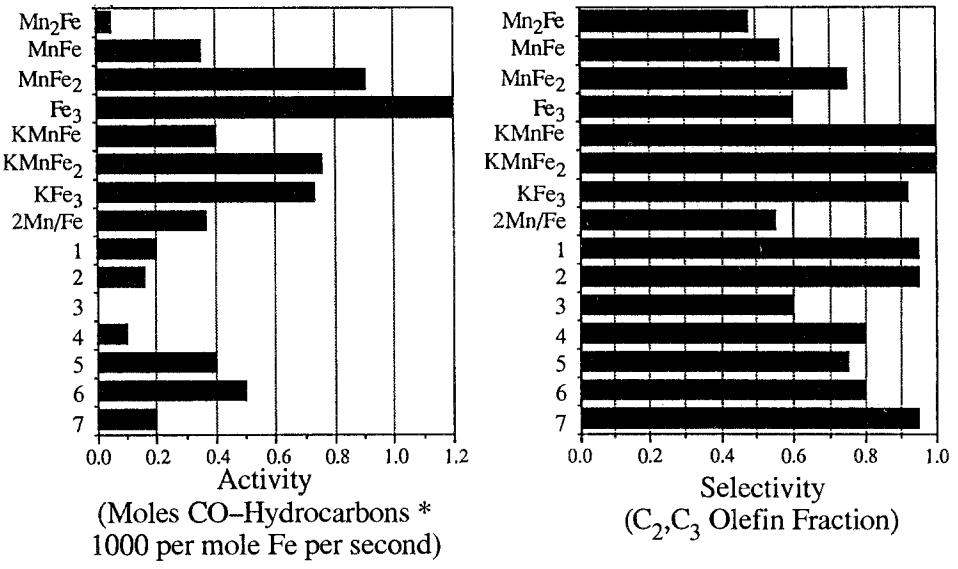

Fig. 1. A comparison of carbon-supported Fe-Mn and K-Fe-Mn catalysts to bulk, and oxide-supported Fe-Mn catalysts: catalytic activities (in millimoles of CO transformed to hydrocarbons per mole Fe per second) and olefin selectivities (olefinic fraction of C_2 and C_3 products).

non-potassium containing catalysts in the original series above. Similarly, two K-containing catalysts were prepared, to correspond with the Fe-containing clusters. The MCC's used for this series of catalysts, the catalyst designations, and the final metal weight loadings (as determined by elemental analysis) are listed in table 3. The Fe weight loadings varied between 5.0 and 8.7%, while the total metal loading varied between 6.5 and 10.2%.

The dispersions of Fe in the final catalysts were measured by the adsorption of CO at 195 K following both LTR and HTR treatments, as well as following the kinetic evaluations. The results are listed in table 4. Bridge bonded CO (CO: Surface Fe = 0.5) was assumed to calculate the dispersions. Dispersions of

Table 3
The metal carbonyl cluster precursors the catalyst designations, and the final weight loadings achieved in the preparation of carbon-supported Fe-Mn and K-Fe-Mn catalysts

Cluster precursor	Designation	Weight loadings (%)			
		Fe	Mn	K	Total
$Fe_3(CO)_{12}$	Fe_3-A	8.7	–	–	8.7
$Fe_3(CO)_{12}$	Fe_3-B	6.5	–	–	6.5
$NEt_4[Fe_2Mn(CO)_{12}]$	Fe_2Mn	5.0	2.8	–	7.8
$Mn_2(CO)_{10}$	Mn_2	–	8.0	–	8.0
$K[HFe_3(CO)_{11}]$	KFe_3	7.2	–	2.7	9.9
$K[Fe_2Mn(CO)_{12}]$	KFe_2Mn	5.3	3.0	1.9	10.2

Table 4
The dispersions of Fe following a low temperature reduction, high temperature reduction, and kinetic evaluations for a series of K-Fe-Mn/C catalysts. (The dispersions were determined by CO chemisorption measurements at 195 K, assuming CO : Fe = 1 : 2.)

Catalyst	Dispersion of Fe [a]		
	Prior to kinetic measurements		Following kinetic measurements
	LTR	HTR	HTR
Fe_3-A	0.58	0.60	0.48
Fe_3-B	0.76	0.70	0.62
Fe_2Mn	0.14	0.64	0.58
Mn_2	–	–	–
KFe_3	0.24	0.72	0.60
KFe_2Mn	0.22	0.78	0.60

[a] $Fe_{surface}/Fe_{Total}$, assuming CO : $Fe_{surface}$ (195 K) = 1 : 2.

between 0.58 and 0.76 were achieved for the non-K containing samples prior to kinetic experiments, and the Fe_3/C catalysts had high dispersions following both LTR and HTR treatments. Excessive temperatures are not required to decompose the clusters. The Mn promoted Fe catalyst, Fe_2Mn/C, had a calculated dispersion of only 0.14 following LTR, which increased to 0.64 following HTR. Both IR and MES experiments showed that the Fe_2Mn cluster is decomposed following LTR. This low dispersion might therefore be attributed to a blocking effect of the Mn component in these very small particles. The Fe in this very small particle phase segregates from the Mn phase during HTR to yield a very small particle following HTR with the Fe and Mn phases segregated, but still in contact, as will be shown later. The non-K containing catalysts, both prior to and following kinetic experiments, are highly dispersed.

The calculated dispersions for the K-containing catalysts display a different trend. Very low dispersions are calculated following a LTR treatment. These particles, however, are actually small as the MES spectra reveal paramagnetically relaxed particles. Furthermore, TEM measurements fail to show the presence of large particles. These results indicate that highly dispersed K-containing particles are formed following an LTR treatment. The calculated dispersions following HTR are high; however, MES spectra reveal that these particles are actually sintered. Large particles (10 to 20 nm in diameter) are formed during HTR, as will be discussed later. It is not clear at this time why the CO chemisorption measurements at 195 K give unrealistic dispersions for K-containing catalysts.

The results in table 4 indicate that highly dispersed 6–10 wt% Fe-Mn/C catalysts were prepared, and that these catalysts remained highly dispersed following CO hydrogenation runs. The K-Fe-Mn/C catalysts were highly dispersed following LTR, but sintered during an HTR treatment.

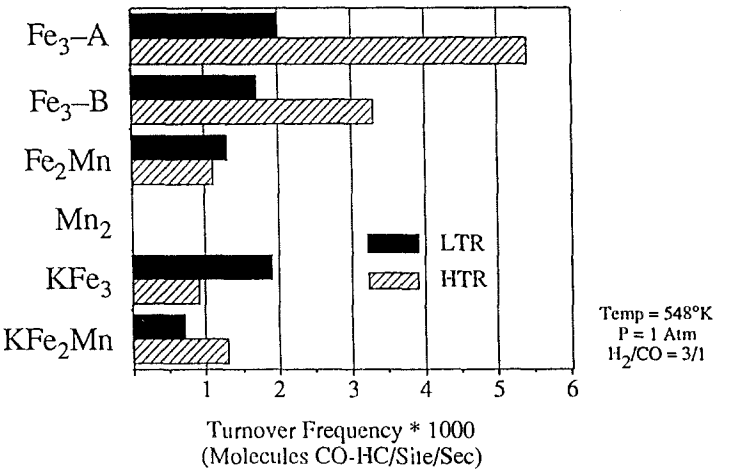

Fig. 2. The turnover frequencies for the hydrogenation of CO to hydrocarbons on a series of carbon-supported Fe-Mn and K-Fe-Mn catalysts.

The CO hydrogenation activities of this series of catalysts are shown in fig. 2. The activities are reported as the turnover frequency (TOF) of CO to hydrocarbons at 548 K, and with a H_2/CO ratio of 3. The surface areas were measured by CO chemisorption at 195 K, as above. All the non-K containing catalysts were active, as TOF's of between 0.001 s^{-1} and 0.005 s^{-1} were measured. The two Fe_3/C catalysts gained activity from the LTR to the HTR treatment, even though the Fe dispersions remained constant. This activation is most probably due to the transformation of Fe from the D-phase particles (as explained later) following LTR to highly dispersed metallic Fe particles following HTR. The Mn promoted catalyst, Fe_2Mn/C, had similar TOF's following LTR and HTR. The K-containing catalysts were also active, with TOF's ranging from 0.0008 to 0.002 s^{-1}. The TOF for KFe_3/C decreased from the LTR to the HTR treatment, while for KFe_2Mn/C the TOF increased from LTR to HTR.

The specific CO hydrogenation activities, in millimoles of CO converted per total moles of Fe per second, are shown in fig. 3. The activities of all the catalysts increased from the LTR treatment to the HTR treatment, and those results as well as the phase behavior for the Fe_3/C catalysts were given previously. The impact on the selectivity of this transformation of D-phase Fe to metallic Fe during HTR on the olefin selectivity is slight, as the olefin-to-paraffin ratio (OPR) remained constant between 1 and 2. The Mn-promoted catalyst, Fe_2Mn/C, also activated in a similar fashion. The OPR of this catalyst dropped from a value of around 5 following LTR to between 1 and 2 following HTR, and the selectivity of this catalyst following HTR was identical to that of the Fe_3/C catalysts. Following LTR, however, this catalyst was very olefin selective. This high olefin selectivity is due to the interaction of Fe and Mn in the highly dispersed particle, either in the bulk or on the surface. As will be explained later, the changes in the

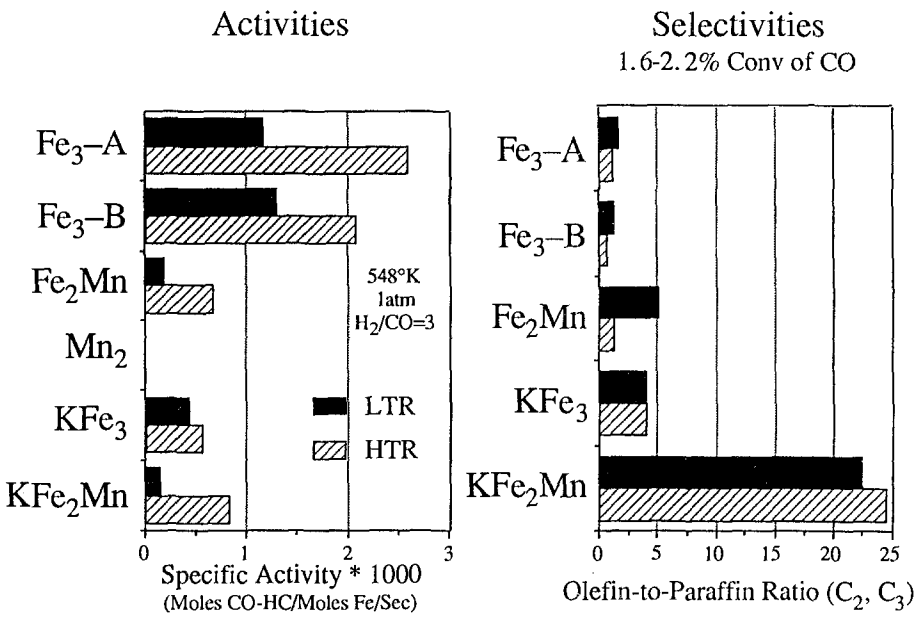

Fig. 3. The specific activities and olefin selectivities of a series of carbon-supported Fe-Mn and K-Fe-Mn catalysts.

activity and selectivity are attributed to the surface of the catalyst becoming more iron-like following HTR. The Fe and Mn phases segregate during HTR, but remain in contact in very small particles.

The K-promoted catalysts have very high selectivities for the formation of low molecular weight olefins. The K-promoted Fe catalyst, KFe_3/C, had an OPR of 4 following both LTR and HTR treatments. The enhancement of selectivity over the unpromoted Fe/C catalyst is therefore due solely to the interaction of K with Fe. The enhancement is not simply due to the highly dispersed nature (small particle sizes) of the catalyst, as the KFe_3/C catalyst sintered significantly during HTR to yield large particles. The activity of the catalyst also remained fairly constant following both LTR and HTR treatments. Similarly, KFe_2Mn/C displayed a particularly high selectivity for light olefins, as OPR's of 22 were measured. This high selectivity was also observed following HTR after the catalyst particles sintered to larger sizes. The selectivity of this catalyst for olefins was higher than that observed for KFe_3/C, indicating that Mn promotion of K-promoted Fe catalysts further enhances selectivities. Again, the enhancement in selectivities can not be explained on the basis of particle size, as small particles were present following LTR but sintered to larger particles following HTR. The enhancement in selectivity is due to the interaction of K and Mn with Fe, and the K and Mn phases therefore have to be in contact with Fe. The activities of both KFe_3/C and Ke_2Mn/C on a per gram Fe basis increased following HTR, indicating that the surface became more iron-like following HTR. This argues for phase segregation within each particle, but with the phases remaining in contact.

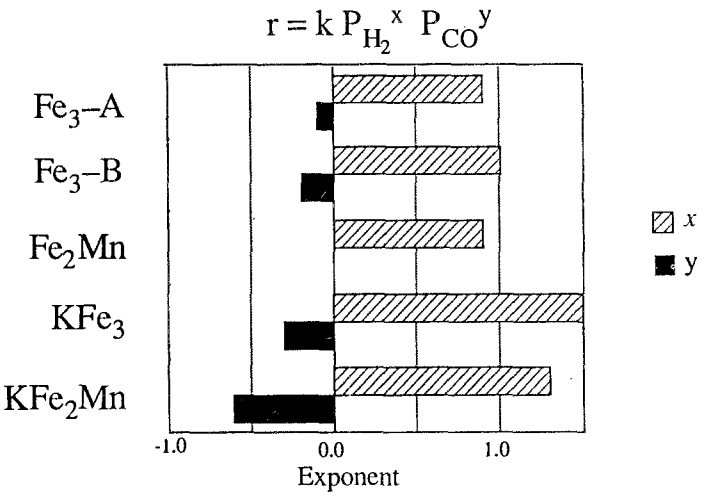

Fig. 4. CO and hydrogen partial pressure dependencies of a series of carbon-supported Fe-Mn and K-Fe-Mn catalysts.

The results from the partial pressure study following an HTR treatment are summarized in fig. 4. The partial pressure dependence for hydrogen was near first order, while the dependence of CO was near zero order for all the catalysts. The partial pressure behavior did not seem to depend very strongly on the nature of the catalyst. This is rather surprising, as the activities and the selectivities of the catalysts varied significantly, even following an HTR treatment. This seems to indicate that the observed differences in the catalytic behavior are due to the differences in the physical states of the catalytic surfaces and not to a change in catalytic mechanism for the different catalysts.

The activation energies (E_a) for the formation of methane were also determined for the series of catalysts, and are shown in fig. 5. First notice that the measured values for each catalyst were rather independent of treatment; for example, the measured values for KFe_3/C following both LTR and HTR were nearly identical. The activation energies for the K-promoted catalysts were higher that those for the unpromoted Fe_3/C catalysts. Interestingly, the E_a values for Fe_2Mn/C hardly varied between LTR and HTR treatments. Considering that the OPR of this catalyst was high [5] following LTR and between 1 and 2 following HTR, one can conclude that the activation energy alone is not sufficient to predict olefin selectivities. However, the high olefin selectivities and high activation energies for the K-promoted catalysts clearly indicate interaction between K and Fe.

The isothermal, integral heats of adsorption of CO (Q_{ads}) were measured for all five catalysts at 300 K following an HTR treatment. The procedures were described elsewhere [23], and consisted of averaging five measurements for each catalyst. These results are also shown in fig. 5. The Q_{ads} values compared very

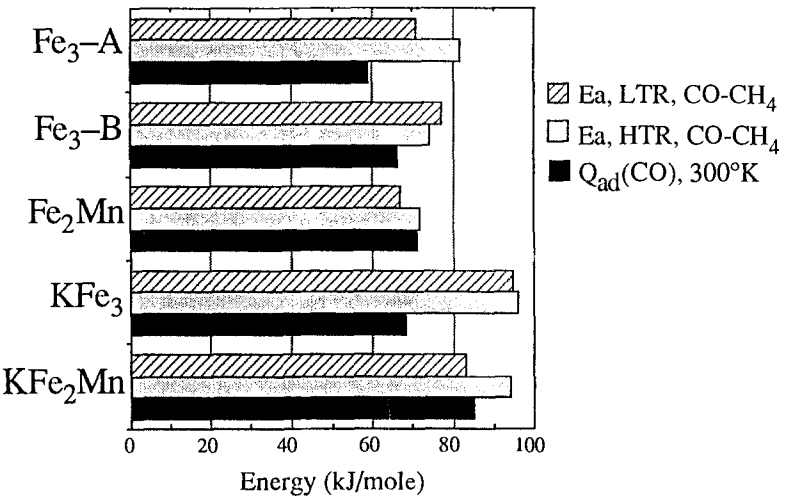

Fig. 5. The activation energies of CO hydrogenation as well as the average, isothermal, integral heats of adsorption of CO of a series of carbon-supported Fe-Mn and K-Fe-Mn catalysts.

favorably with the measured activation energies. The Q_{ads} value measured for the Fe_3/C catalysts (averaged for A and B) was the lowest at 15 kcal/mole. The values for the singly promoted catalysts, Fe_2Mn/C and KFe_3/C, were nearly identical at 17 kcal/mole, while the doubly promoted catalyst, KFe_2Mn/C, had the highest Q_{ads} value of 21 kcal/mole. Again, considering that Fe_2Mn/C had an OPR similar to that of Fe_3/C following HTR, and that KFe_3/C had an OPR similar to that of KFe_2Mn/C following HTR, one can not attribute high olefin selectivities to high Q_{ads} values only; however, the catalyst with the highest Q_{ads} value in this study also had the highest olefin selectivity. The Q_{ads} values do give clear indications that the interaction between Fe and the promoters are real: the singly promoted catalysts have higher Q_{ads} values than Fe_3/C, while the doubly promoted catalyst had the highest value. For this to happen, the promoters have to be in close proximity to the Fe phase following HTR.

B: DRIFTS AND MES STUDY

The second half of the paper will address the physical state of the metal particles in more detail. A sequential analysis will be given, where the state of the catalysts following each pretreatment stage is described and related to the catalytic activity.

B.1. Impregnation

The state of the catalysts directly following impregnation is of interest. In order to establish what the MCC-carbon interactions are at this early stage, DRIFTS and MES spectra were collected on the freshly prepared catalysts. DRIFTS, recently developed to allow the study of clusters on carbons [40], was

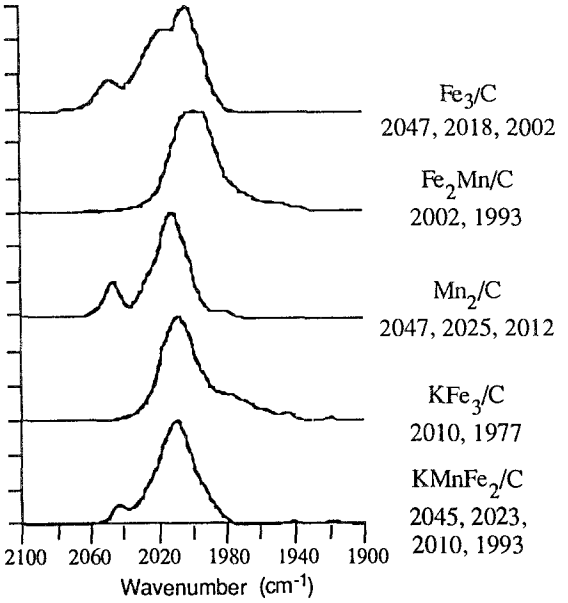

Fig. 6. DRIFTS spectra of carbon-supported Fe-Mn and K-Fe-Mn clusters. The spectra of the freshly prepared catalysts were collected in flowing He at 300 K.

used to identify the supported clusters. These spectra are shown in fig. 6. The observed carbonyl stretching frequencies are very similar to those observed for the clusters in solution [19]. It indicates that the clusters remain intact following impregnation, except for $Fe_3(CO)_{12}$ which partly decomposes to $Fe(CO)_5$. Significant amounts of the clusters are still present following impregnation. The MES spectra, collected at 77 K, of three supported clusters are shown in fig. 7. These spectra lead to a similar observation: the clusters remain intact during impregnation and exist as such on the carbon surface. No indication of oxidized Fe or metallic Fe was present in the MES spectra.

The above results indicate clearly the differences that exist between carbon surfaces and oxide supports. On oxide supports $Fe_3(CO)_{12}$ readily transforms to anionic clusters during impregnation due to surface hydroxyl groups [19,20]. On treated carbons, these groups are specially reduced to prevent the oxidation of small metallic Fe particles. Furthermore, since the clusters remain intact during impregnation, carbon surfaces provide an unique opportunity to study cluster behavior in two dimensions.

B.2. Cluster decomposition

A thorough description of the decomposition of all the supported clusters is given elsewhere [19–21]. The decomposition of the catalysts was followed by both DRIFTS and MES. The characterization of a single catalyst by each technique will be described here for illustrative purposes.

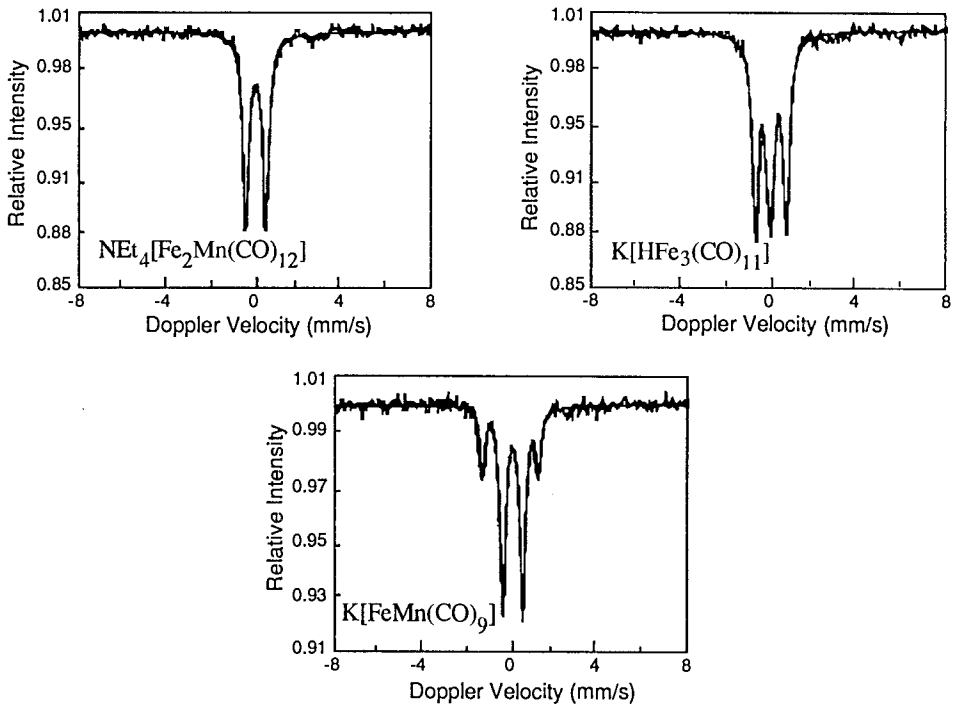

Fig. 7. MES spectra of carbon-supported Fe-Mn and K-Fe-Mn clusters. The spectra of the freshly prepared catalysts were collected at 77 K.

The decomposition of $NEt_4[Fe_2Mn(CO)_{12}]/C$ in hydrogen, as studied by MES, is shown in fig. 8. The freshly impregnated catalyst was heated to 323 K for 1 hour, then cooled to 77 K for analysis. Following this, it was heated to 373 K for 1 hour, cooled, and analyzed. In this way spectra were obtained for four stages of decomposition. The first spectrum, after 1 h at 323 K, indicates that the cluster remains intact. More severe treatments, 1 h at 373 K and an additional hour at 423 K, transform the original cluster into one with a spectrum shown in fig. 8. Based on this spectrum and DRIFTS spectra, this new cluster is $[HFe_4(CO)_{13}]^-$. This cluster then decomposes during a 1 hour treatment in hydrogen at 473 K, yielding the spectrum of highly dispersed Fe present in the D-phase [20].

The decomposition of a very similar cluster, $K[Fe_2Mn(CO)_{12}]/C$, in hydrogen as studied by DRIFTS is shown in fig. 9. The original spectrum indicates the presence of two cluster species, $[MnFe_2(CO)_{12}]^-$ and $Mn_2(CO)_{10}$. This cluster then decomposes very slowly at 308 K to yield the final spectrum after 1080 minutes, again showing the presence of two species, $Mn_2(CO)_{10}$ and $[HFe_4(CO)_{13}]^-$ [19].

The above two series of experiments demonstrate that the original, intact clusters slowly disintegrate during decomposition. The products of this decom-

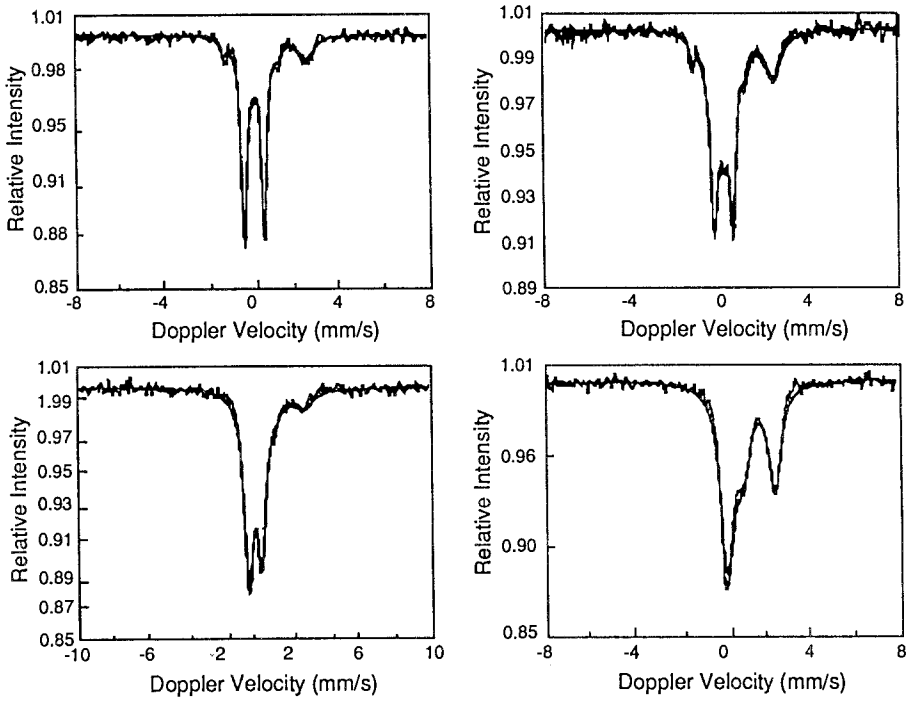

Fig. 8. MES spectra of carbon-supported $NEt_4[Fe_2Mn(CO)_{12}]$. Spectra were collected at various stages during the decomposition in hydrogen.

position are monometallic species, namely $Mn_2(CO)_{10}$ and $[HFe_4(CO)_{13}]^-$. Although these clusters are monometallic, they are in very close proximity, ultimately decomposing to yield MnO_x and Fe (D-phase) within a single particle.

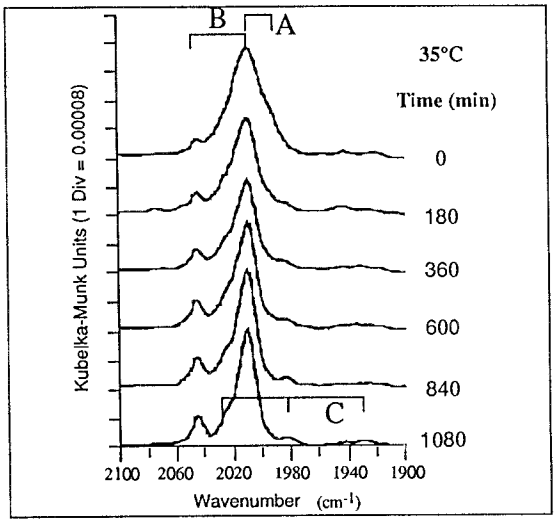

A = $[MnFe_2(CO)_{12}]^-$

B = $[Mn_2(CO)_{10}]$

C = $[HFe_4(CO)_{13}]^-$

Fig. 9. DRIFTS spectra of carbon-supported $K[Fe_2Mn(CO)_{12}]$. Spectra were collected at 308 K in flowing hydrogen.

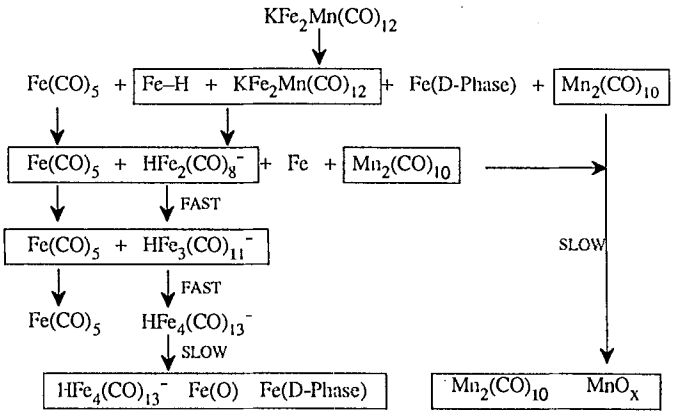

Fig. 10. The mechanism of decomposition of carbon-supported $K[Fe_2Mn(CO)_{12}]$.

The two promoter phases within this single particle (MnO_x and K) are then able to alter the catalytic properties of the final catalyst as described above. A schematic summary of the proposed decomposition mechanism is given in fig. 10, and is more fully described elsewhere [19–21].

B.3. Following low temperature reduction

MES spectra of the catalysts at 77 K following decomposition at 473 K are shown in fig. 11. The spectrum for supported Fe_3/C is not shown, but is very similar to that shown for $NEt_4[Fe_2Mn(CO)_{12}]$ [20]. Notice that all five catalysts following decomposition have very similar spectra, namely that of Fe present in the D-phase [20]. The nature of this D-phase is discussed in detail elsewhere [20]. The spectra for all the catalysts, including the K-promoted catalysts, are relaxed, indicating that very small particles are present following an LTR treatment.

It is interesting to note that the spectra of Fe_2Mn/C and Fe_3/C following LTR are nearly identical, yet that the catalytic behavior is significantly different: Fe_2Mn/C has a much higher selectivity for olefins than Fe_3/C. Considering that MES is a technique that probes the bulk composition of particles, it can be concluded that states of the bulk Fe present in these two catalysts are very similar. As the olefin selectivities are significantly different, the catalytic surfaces of these two catalysts must be different due to the presence of MnO_x as a promoter. Since these modifications in the surfaces of the particles can not be observed by MES even for these highly dispersed particles, one can conclude that only a very small fraction of the Fe present is modified.

The potassium-promoted catalysts remain highly dispersed following LTR. The spectra for these catalysts appear different from the Fe_3/C and Fe_2Mn/C catalysts, as the side peak has a higher intensity. This side peak is probably due to a highly dispersed iron oxide or carbide [21]. Although it is tempting to correlate the intensity of this side peak with the olefin selectivity following LTR, the

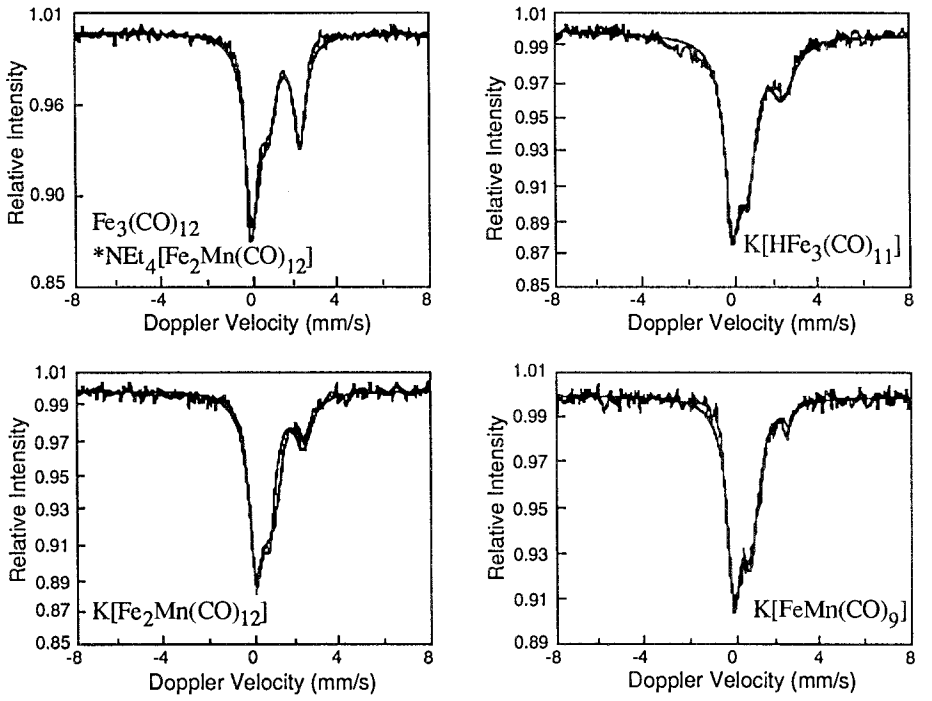

Fig. 11. MES spectra of carbon-supported Fe-Mn and K-Fe-Mn catalysts following an LTR treatment. (The spectra were collected for the catalysts denoted by an asterisk.)

observation that this intensity for Fe_3/C and for Fe_2Mn/C was nearly identical argues strongly against such a correlation. This side peak seems to be more meaningful when interpreted in terms of the distribution of bulk Fe phases present, rather than the composition of the olefin selective surface.

Attempts were made to obtain the DRIFTS spectra of adsorbed CO on the catalysts following LTR treatments. All the attempts failed to indicate the presence of bridged or linearly adsorbed CO, as well as carbonyl species. The chemisorption measurements, however, show that very large amounts of CO adsorbed on the catalysts. These adsorbed species should have been detected by DRIFTS, as carbonyls at similar concentrations and CO adsorbed following HTR, can be easily detected. These results imply strongly that the CO adsorbed following an LTR treatment is adsorbed in an IR-inactive form, for example as a highly tilted or flat lying species [19–21], or it can also dissociate. This tilted species would result if the CO adsorbed on Fe, with the oxygen end interacting with the promoter present on the same particle. This interaction is entirely possible on unpromoted Fe surfaces also, as similar tilted species have been observed for rough (open) Fe single crystals [41]. While tilted species can exist on both promoted and unpromoted supported Fe catalysts, the species with which the oxygen end of CO interacting may be profoundly affected in regard to the ease with which the C-O bond is broken due to the differences in the heats of

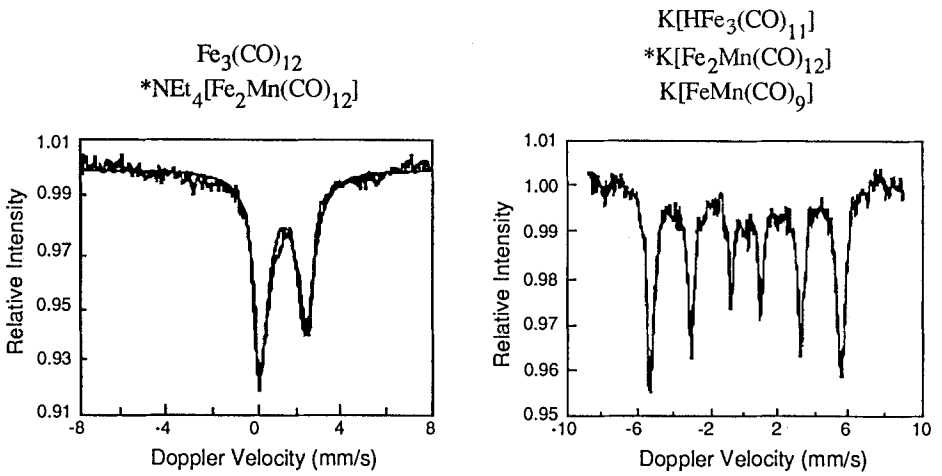

Fig. 12. MES spectra of carbon-supported Fe-Mn and K-Fe-Mn catalysts following an HTR treatment. (The spectra were collected for the catalysts denoted by an asterisk.)

adsorption of oxygen on the Fe, Mn, and K phases [42]. This, in turn, could markedly affect the resulting activities and selectivities. The extent of this interaction will depend very strongly on the proximity of the promoter, and therefore on the pretreatment of the catalyst. Although quantification of this interaction is beyond the scope of this work, it may explain to some extent the variations in catalytic properties described above.

B.4. Following high temperature reduction

The MES spectra of the catalysts following an HTR treatment are shown in fig. 12. Only two spectra are shown, namely those for Fe_2Mn/C and KFe_2Mn/C, because the spectrum for Fe_3/C is very similar to the former and those for KFe_3/C and KFeMn/C are similar to the latter.

The spectra for Fe_3/C and Fe_2Mn/C indicate that both of these catalysts remained highly dispersed following HTR, as particles containing Fe present in a magnetically relaxed state at 77 K were obtained. In addition, the D-phase character of the iron phase was retained. These particles are rather resistant to sintering, as confirmed by the high dispersions measured by CO chemisorption measurements.

The spectra for the K-promoted catalysts changed markedly during the HTR treatment because the highly dispersed D-phase particles sintered, thus forming large metallic Fe particles. The alfa-iron spectra obtained is clear evidence of this.

The relation between the physical state of the catalysts and the catalytic behavior is illustrated further here. The kinetic behavior for Fe_3/C did not change markedly from LTR to HTR, and neither did the MES spectrum. Although the MES spectrum for Fe_2Mn/C did change slightly (disappearance of the side peak), the olefin selectivity changed markedly. Similarly, the MES

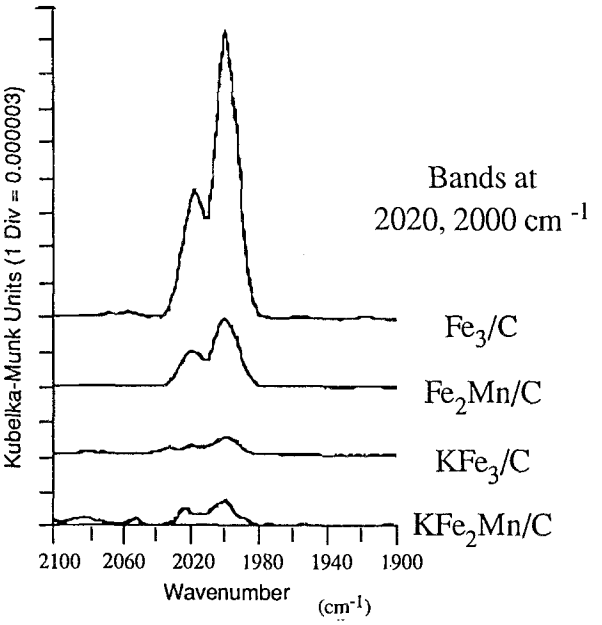

Fig. 13. DRIFTS spectra of adsorbed CO on carbon-supported Fe-Mn and K-Fe-Mn catalysts at 300 K following an HTR treatment.

spectra for the K-promoted catalysts changed dramatically from LTR to HTR treatments, but their catalytic properties hardly changed. Consequently there appears to be no correlation between the MES spectra and the catalytic properties. This demonstrates very clearly that the catalytic behavior is determined by the surface properties of the catalysts, and that the MES spectra mainly probe the bulk properties; however, it also demonstrates that highly active and selective catalysts can be prepared for a variety of bulk compositions.

The differences between the surface properties of the above catalysts can be demonstrated by the DRIFTS spectra of adsorbed CO, as shown in fig. 13. Spectra were obtained for Fe_3/C, Fe_2Mn/C, KFe_3/C, and KFe_3/C. All three catalysts had identical spectra, as only bands that can be associated with $Fe(CO)_5$ were observed. For Fe_3/C, a significant amount of $Fe(CO)_5$ was reformed during CO adsorption at 300 K. This is indicative of the presence of very highly dispersed, metallic Fe particles following HTR [19–21]. This intensity for Fe_2Mn/C was significantly reduced. The presence of MnO_x in these equally highly dispersed particles prevents the formation of $Fe(CO)_5$ upon CO adsorption, thus the MnO_x phase has to be in close contact with the surface Fe atoms. The K-promoted catalysts show almost no reformation of $Fe(CO)_5$, as would be expected for these large Fe particles.

It is interesting that IR bands for linearly and bridged CO species were not observed for any of these catalysts following HTR. This is most probably due to

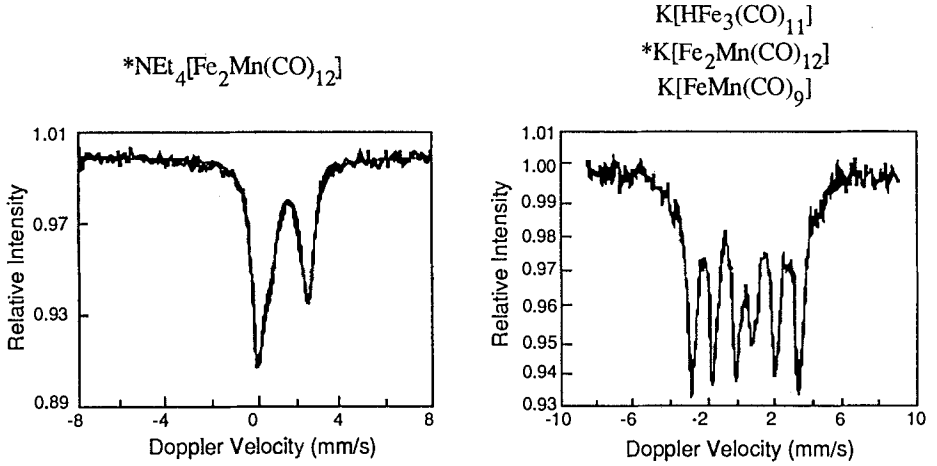

Fig. 14. MES spectra of carbon-supported Fe-Mn and K-Fe-Mn catalysts following 2 hours of syngas flow at 498 K (H_2-to-CO = 3).

CO dissociation or to the CO being present in an IR inactive form, as described above.

B.5. Following CO hydrogenation

The MES spectra of the catalysts above following a two hour exposure to synthesis gas (H_2 : CO = 3 : 1) at 498 K are shown in fig. 14. The spectra were collected at 77 K. The Fe_2Mn/C catalyst retained its high dispersion following reaction conditions, and, addition, the Fe remained in the D-phase. The Fe_3/C and Fe_2Mn/C catalysts were very resistant to sintering, as the average particle size remained very small. No evidence for the formation of carbidic Fe was found. The spectra for the K-promoted catalysts are also shown in fig. 14. All three catalysts carburized rapidly and completely to ϵ'-carbide, as would be expected for large alfa-iron particles. It is important to notice that these three catalysts retained their high activities and olefin selectivities for the duration of the 2 hours. The transformation of the bulk Fe phase from alfa-iron to ϵ'-carbide had no significant effect on either the activity or the selectivity. The active and selective surface sites apparently remained unaltered. It has been reported that alfa-iron particles, even when highly dispersed, can readily carburize [13,20,34,44], but when Mn is incorporated in the Fe phase carbide formation is suppressed [6,12,15]. Small amounts of Mn appear to have been incorporated in the Fe phase for Fe_2Mn/C, while no Mn was incorporated in the bulk Fe phase (alfa iron) for K-promoted catalysts; however, since the catalytic properties of the K-promoted catalysts were clearly different from those of Fe_3/C, both the K and MnO_x promoters appear to be in close contact with the Fe phase.

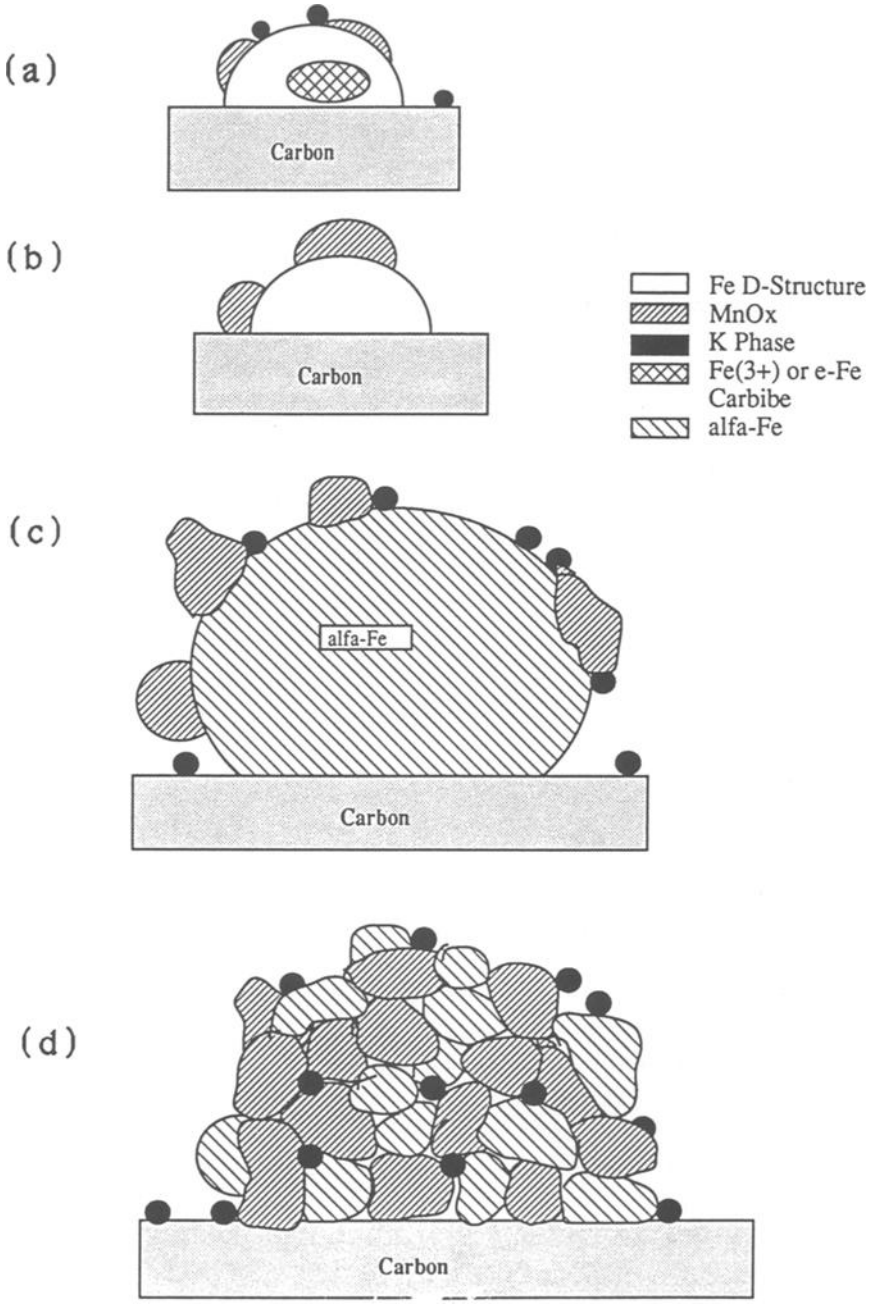

Fig. 15. (a) Proposed state of K-Fe-Mn/C catalysts after LTR; Fe-Mn/C catalysts are presumed to be similar, only the K phase is absent. The iron particles are small (< 4 nm), and exist primarily in the D-structure. (b) Proposed state of Fe-Mn/C catalysts after HTR. The Fe particles remain small and exist in the D-structure, and the Mn oxide has sintered into three-dimensional particles. (c) One possible state of the K-Fe-Mn/C catalysts after HTR. The iron has sintered, along with the Mn oxide, to form large ferromagnetic alfa-iron (> 30 nm) crystallites. (d) Alternate state of the K-Fe-Mn/C catalysts after HTR. Small zero-valent iron phases are mixed with MnO_x phases to form a larger composite particle. Because of their proximity and the interaction anisotropy these Fe particles give a Mössbauer spectrum comparable to that of ferromagnetic alfa-iron crystallites.

B.6. Proposed model

A model for the evolution of K-Fe-Mn/C catalysts is proposed to explain all the observations, and is illustrated in fig. 15. Following a LTR treatment the Fe-Mn/C catalysts are present as highly dispersed metal particles, with the Fe present as a D-structure. The Mn is present on the surface of these particles as thin MnO_x layers. Small amounts of Fe(3 +) or ϵ-carbide may be present on the surface, which may affect the catalytic properties, but remained undetected in this study. The K-Fe-Mn/C catalysts following LTR treatments resemble the above, but also have a K-phase present.

The Fe-Mn/C catalysts remain highly dispersed following an HTR treatment, with the Fe still present in the D-structure. The Mn-oxide phase sintered to some degree to form larger structures in contact with the Fe phase. The smaller contact area with the Fe phase leads to a lowering of the olefin selectivity. The K-Fe-Mn/C catalysts sintered significantly during HTR treatments, yielding large alfa-Fe particles, and in contact with these particles are the K and sintered MnO_x phases. The contact between the Fe and K phases leads to the observed enhancement in olefin selectivities.

4. Summary and conclusions

The evolution of Fe-Mn/C and K-Fe-Mn/C catalysts has been studied from the stages of impregnation to the final state following CO hydrogenation. A reaction sequence for Fe_2Mn/C and KFe_2Mn/C cluster decomposition is proposed based on MES and DRIFTS results, taking into account solution chemistry studies. In the absence of K, either a LTR or a HTR treatment produces highly dispersed Fe catalysts. Addition of K to the clusters results in considerable particle growth during HTR. Despite this, the surfaces of the K-promoted and doubly promoted (K and Mn) LTR and HTR samples under reaction conditions produce similar catalytic behavior in most aspects, at least under low conversions where reducing conditions are maintained, as OPR and TOF's were comparable. The CO heats of adsorption on these catalysts after HTR indicated that the addition of either Mn or K increased Q_{ads} values, and this effect was additive as the doubly promoted sample gave the highest value, with an increase in Q_{ads} close to the sum of the increments produced by the two promoters separately. This implies that the Mn and K phases are in contact with the Fe surface atoms, and it is likely that the phases containing K and Mn are in direct contact with each other as well as the iron surface.

Acknowledgments

This study was supported by the National Science Foundation under Grant CBT-8619619. The Mössbauer effect spectroscopic study was conducted by Dr. Andrew Chen and Dr. Jonathan Phillips.

References

[1] S.L. Soled and R.A. Fiato, U.S. Patent 4, 604, 375 (1986).
[2] R.A. Fiato and S.L. Soled, U.S. Patent 4, 621, 102 (1986).
[3] K.B. Jensen and F.E. Massoth, J. Catal. 92 (1985) 98.
[4] K.B. Jensen and F.E. Massoth, J. Catal. 92 (1985) 109.
[5] M.G. Zhuravleva, G.I. Chufarov and D.Z. Brainina, Dokl. Acad. SSSR. 132 (1960) 1074.
[6] U. Lochner, H. Papp and M. Baerns, Appl. Catal. 23 (1986) 339.
[7] J. Barrault, C. Renard, L.T. Yu and J. Gal, in: *Proc. 8th Int. Cong. on Catalysis*, Berlin, 1984 (Dechema, Frankfurt-am-Main, 1984) Vol. 2, p. 101.
[8] T. Gryzbek, H. Papp and M. Baerns, Appl. Catal. 29 (1987) 335.
[9] J.M. Stencel, J.R. Diehl, S.R. Miller, R.A. Anderson, M.F. Zarochak and H.W. Pennline, Appl. Catal. 33 (1987) 129.
[10] J. Barrault and C. Renard, Appl. Catal. 14 (1985) 133.
[11] N.K. Jaggi, L.H. Schwartz, J.B. Butt, H. Papp and M. Baerns, Appl. Catal. 13 (1985) 347.
[12] G.C. Maiti, R. Malessa and M. Baerns, Appl. Catal. 5 (1983) 151.
[13] G.C. Maiti, R. Malessa, U. Lochner, H. Papp and Baerns, M., Appl. Catal. 16 (1985) 215.
[14] P. Deppe, H. Papp and M. Rosenberg, Hyp. Int. 28 (1986) 903.
[15] G. Lohrengel and M. Baerns, Ber. Bunsen. Ges. Phys. Chem. 87 (1983) 335.
[16] L. Bruce, G. Hope and T.W. Turney, React. Kinet. Catal. Lett. 20 (1982) 175.
[17] V.L. Kuznetsov, H.F. Danilyuk, I.E. Kolosova and Y.I. Yermakov, React. Kinet. Catal. Lett. 21 (1982) 249.
[18] J. Venter, M. Kaminsky, G.L. Geoffroy and M.A. Vannice, J. Catal. 103 (1987) 450; 105 (1987) 155.
[19] J.J. Venter, A. Chen and M.A. Vannice, J. Catal. 117 (1989) 170.
[20] A.A. Chen, J. Phillips, J.J. Venter and M.A. Vannice, J. Catal. 118 (1989) 443.
[21] J.J. Venter, A.C. Chen, J. Phillips and M.A. Vannice, J. Catal. 119 (1989) 451.
[22] J.J. Venter, M. Kaminsky, G.L. Geoffroy and M.A. Vannice, in: *Preparation of Catalysts*, IV, eds. B. Delmon et al. (Elsevier, Amsterdam, 1987) p. 479.
[23] J.J. Venter and M.A. Vannice, J. Phys. Chem. 93 (1989) 4158.
[24] H.J. Jung, P.L. Walker and M.A. Vannice, J. Catal. 75 (1982) 416.
[25] M.A. Vannice, P.L. Walker, H.J. Jung, C. Moreno-Castilla and O.P. Mahajan, *Proc. 7th Intl. Cong. Catal.* (Elsevier, Amsterdam, 1981) p. 460.
[26] P.H. Emmett and S. Brunauer, J. Amer. Chem. Soc. 59 (1937) 310.
[27] M.A. Vannice, J. Catal. 37 (1975) 449.
[28] B. Sen, P. Chou and M.A. Vannice, J. Catal. 101 (1986) 517.
[29] S.C. Lin and J. Phillips, J. Appl. Phys. 58 (1985) 1943.
[30] J. Barrault, Y.C. Forquy and V. Perrichon, Appl. Catal. 5 (1983) 119.
[31] J. Barrault and C. Renard, Appl. Catal. 14 (1985) 133.
[32] W.D. Deckwer, H.J. Lehmann, M. Ralek and B. Schmidt, Chem. Ing. Tech. 53 (1981) 818.
[33] W.D. Deckwer and Y. Serpemen, I&EC Process. Des. Dev. 21 (1982) 222.
[34] W.L. Van Dijk, J.W. Niemantsverdriet, A.M. van der Kraan and H.S. Van der Baan, Appl. Catal. 2 (1982) 273.
[35] C.N. Satterfield and H.G. Stenger, I&EC Process. Des. Dev. 23 (1984) 26.
[36] C.N. Satterfield and G.A. Huff, J. Catal. 85 (1984) 370.
[37] H. Schulz and H. Gockebay, in: *9th Conf. on Catal. of Org. React.*, Charleston, SC, USA, April, 1982.
[38] H. Schulz, in: *5th Intl. Conf. on Het. Catal.*, Varna, Bulgaria, Oct. 3-4, 1983.
[39] W. Benecke, H. Schulz, H.G. Feller and M. Ralek, in: *Proc. 8th Int. Cong. on Catalysis*, (Dechema, Frankfurt, 1985). Vol. 4, p. 219.

[40] J.J. Venter and M.A. Vannice, J. Amer. Chem. Soc. 109 (1987) 6204; Appl. Spectrosc. 42 (1988) 1096; Carbon 26 (1988) 889.
[41] J.J. Venter and M.A. Vannice, J. Phys. Chem. 93 (1989) 4158;
U. Seip, M.C. Tsai, K. Cristman, J. Kuppers and G. Ertl, Surf. Sci. 139 (1984) 29;
D.W. Moon, S.L. Bernasek, J.P. Lu, J.L. Gland and D.J. Dwyer, Surf. Sci. 184 (1987) 90;
J. Amer. Chem. Soc. 107 (1985) 4363.
[42] E. Scustorovich, Acc. of Chem. Res. 21 (1988) 183;
E. Schustorovich and A.T. Bell, J. Catal. 113 (1988) 341;
A.T. Bell and E. Schustorovich, J. Catal. 121 (1990) 1.
[43] A.A. Chen, M.A. Vannice and J. Phillips, J. Phys. Chem. 91 (1987) 6257.
[44] J.W. Niemantsverdriet, A.M. van der Kraan, W.N. Delgass and M.A. Vannice, J. Phys. Chem. 89 (1985) 67.